Published in final edited form as:
Dev Cell. 2011 November 15; 21(5): 907–919. doi:10.1016/j.devcel.2011.08.027.

Anterior Visceral Endoderm Directs Ventral Morphogenesis and Placement of Head and Heart via BMP2 Expression

Mary Madabhushi and **Elizabeth Lacy**
Developmental Biology Program, Sloan-Kettering Institute, New York, NY 10065 USA, Weill Graduate School of Medical Sciences of Cornell University, New York, NY 10065 USA

SUMMARY

In amniotes ventral folding morphogenesis achieves gut internalization, linear heart tube formation, ventral body wall closure, and encasement of the fetus in extraembryonic membranes. Impairment of ventral morphogenesis results in human birth defects involving body wall, gut, and heart malformations and in mouse misplacement of head and heart. Absence of knowledge about genetic pathways and cell populations directing ventral folding in mammals has precluded systematic study of cellular mechanisms driving this vital morphogenetic process. We report tissue-specific mouse mutant analyses identifying the Bone Morphogenetic Protein (BMP) pathway as a key regulator of ventral morphogenesis. BMP2 expressed in anterior visceral endoderm (AVE) signals to epiblast derivatives during gastrulation to orchestrate initial stages of ventral morphogenesis; including foregut development and positioning of head and heart. These findings identify unanticipated functions for the AVE in organizing the gastrulating embryo and indicate that visceral endoderm-expressed BMP2 coordinates morphogenetic cell behaviors in multiple epiblast lineages.

INTRODUCTION

Following implantation at embryonic day (E) 4.5, an extraembryonic cell layer, the visceral endoderm (VE), encases the entire mouse embryo, a radially symmetric cylinder consisting of the epiblast distally and the extraembryonic ectoderm (ExE) proximally. Before the onset of gastrulation, marked by primitive streak formation at E6.25, the VE acts as a multi-functional tissue, mediating nutrient-waste exchange between the maternal circulation and the growing embryo, while also delivering signals to position the body axis and initiate anterior patterning (Arnold and Robertson, 2009; Mao et al., 2010). During gastrulation (~6.5 - E8) the VE forms the endodermal layer of the yolk sac and continues to coordinate nutrient uptake and waste exchange. Whether the VE also continues to provide organizing signals that position and pattern the three primary germ layers generated during gastrulation remains unknown; this is the central question investigated in our studies.

The distal visceral endoderm (DVE), a morphologically distinct population of embryonic VE (EmVE) cells generated at the distal end of the E5.5 conceptus (Arnold and Robertson, 2009; Rivera-Perez et al., 2003), executes the key organizer activities of the VE prior to gastrulation. The DVE migrates proximally to the junction between the prospective anterior

Contact: Elizabeth Lacy, e-lacy@mskcc.org; 212-639-7538 phone; 646-422-2062 FAX.

epiblast and ExE, giving rise to the AVE by E5.75-E6.0 (Srinivas et al., 2004; Thomas and Beddington, 1996). During its migration, the DVE/AVE secretes inhibitors that restrict WNT and NODAL signaling, and consequently primitive streak formation, to the most proximal epiblast at the future posterior side of the embryo (Kimura-Yoshida et al., 2005; Perea-Gomez et al., 2002). Concurrently, these inhibitors confer a neurectodermal identity to overlying anterior epiblast (Perea-Gomez et al., 1999; Rhinn et al., 1998).

Studies on the origin and morphogenesis of the definitive endoderm (DE) cell lineage led to the predominant model that a steady production of nascent endoderm cells by the anterior primitive streak expands and propels a contiguous layer of DE cells proximally, until the EmVE, including the AVE, is displaced into the extraembryonic region at E7.5 (Arnold and Robertson, 2009; Lawson and Pedersen, 1987). Since such an extraembryonic position would separate the EmVE/AVE from the embryo proper, it has been assumed that the EmVE/AVE could not influence embryonic patterning once gastrulation had initiated. However, a recent study has led to a significant revision of this model for endoderm formation (Kwon et al., 2008; Nowotschin and Hadjantonakis, 2010). By tracking genetically labeled VE cells during gastrulation, Kwon et al (2008) documented the rapid dispersal of EmVE cells by a multifocal intercalation of DE cells. Rather than becoming displaced to the extraembryonic region, the EmVE cells combined with the DE cells to form a single epithelium. Moreover, the EmVE derivatives persisted within the gut tube until at least the 20 somite stage, E9.0-E9.5. Importantly, their location in the embryonic region, interspersed with streak derived endoderm cells and adjacent to mesodermal and ectodermal populations, indicates that EmVE cells are positioned to continue functioning as regulators of tissue patterning and morphogenesis during and following gastrulation. The studies reported herein document a regulatory role of the VE lineage in tissue morphogenesis after primitive streak formation and generation of the definitive germ layers.

In response to NODAL signaling at E5.25-E5.5, before DVE formation, the EmVE and ExVE start to display different gene expression profiles (Mesnard et al., 2006). Among the EmVE-specific genes is *Bmp2*. Subsequently, at the early primitive streak stage (ES, ~E6.25-E6.5), *Bmp2* expression persists in the EmVE and one study, based on embryo morphology, localized *Bmp2* transcripts to the posterior region of the EmVE (Ying and Zhao, 2001). Despite its established expression in the VE, it has remained unclear whether EmVE-derived BMP2 plays a requisite role during the pre-streak and gastrulation stages. In fact, when the phenotype of $Bmp2^{-/-}$ (KO) embryos was first described, *Bmp2* was not known to be transcribed in the VE. Consequently, the phenotypic defects affecting formation of the amnion and heart were ascribed exclusively to the loss of BMP2 expression from extraembryonic and cardiac mesoderm (Zhang and Bradley, 1996).

We investigated a requirement for BMP2 expression in the VE by applying Cre-lox recombination to separately delete *Bmp2* from the VE and epiblast cell lineages. Here we show that after primitive streak formation VE-expressed BMP2 performs a pivotal and previously unknown role in directing ventral folding morphogenesis in the anterior region of the embryo. Through a detailed examination of temporal and spatial patterns of gene transcription, we establish that BMP2 is expressed in a discrete subset of AVE cells and not in the posterior EmVE as reported. Together these findings define an unanticipated late function for the AVE. Acting during the neural plate and early head fold (EHF) stages (E7.5-E8.0), the AVE regulates the initial steps of ventral morphogenesis, including foregut development and positioning of head and heart. The AVE executes its role in ventral folding through the expression of BMP2, which signals to epiblast-derived tissues to coordinate morphogenetic cell behaviors.

RESULTS

Bmp2 Transcription Localizes to the Proximal AVE during Gastrulation

Previous studies on *Bmp2* expression examined VE at the pre-to-early streak stages (E5.5-E6.5) (Coucouvanis and Martin, 1999; Mesnard et al., 2006; Stuckey et al., 2011; Yamamoto et al., 2009; Ying and Zhao, 2001) or extraembryonic mesoderm, cardiac progenitors, and surface/neural ectoderm at head fold stages (HF, E8.0-E8.5) (Biben et al., 1998; Fujiwara et al., 2002; Kanzler et al., 2000; Winnier et al., 1995; Zhang and Bradley, 1996). These studies excluded the neural plate stages at ~E7.5 when the *Bmp2* mutant phenotype first emerges (Zhang and Bradley, 1996). To evaluate which, if any, of the phenotypic defects in the $Bmp2^{-/-}$ mutant result directly from the loss of BMP2 expression in VE, we documented the spatial distribution of *Bmp2* transcripts in both VE and epiblast-derived tissues in wild-type (WT) embryos between E5.0 and E8.0. (Figure S1a diagrams the criteria we used to define the developmental stage of embryos dissected at gestational days E5.5-to-E8.0.) In pre-streak (PS) embryos, at both DVE and AVE stages (~E5.5), *Bmp2* was expressed throughout the EmVE (Figure 1A, Figure S1bA-S1bD). We distinguished between DVE and AVE stages by the location of *Hex*-GFP fluorescence at, respectively, the distal tip or anterior VE (Rodriguez et al., 2005) (Figure S1a; Figure S1bA-S1bD). Early streak (ES) embryos exhibited a broad distribution of *Bmp2* transcripts in the proximal region of the EmVE, with the highest levels anteriorly (Figure S1bE-S1bF). By mid-streak (MS), *Bmp2* expression was confined to a patch of cells in the proximal-most anterior VE (Figure 1B, 1G). We verified the anterior position of *Bmp2* transcripts at the ES-MS stages (~E6.5) by two-color *in situ* hybridization for *Bmp2* and either *Cer1* or *brachyury*. *Bmp2* expression overlapped with *Cer1*, an AVE marker, opposite from the *brachyury*-expressing streak cells (Figure 1F). *Bmp2* expression in anterior endoderm persisted through the late head fold (LHF) stage at ~E8.0 (Figure 1C-1E).

Bmp2 is Transcribed in the Ventral Node and Anterior Midline as well as in Cardiac and Extraembryonic Mesoderm

We first detected *Bmp2* transcripts in epiblast lineages at E7.5 during the neural plate stages (OB-no allantoic bud, EB-early allantoic bud, LB-late allantoic bud); nearly two days after the onset of expression in the VE. OB-EB stage embryos expressed *Bmp2* in the ventral node and anterior midline; EB embryos also contain *Bmp2* in anterior wing mesoderm spanning the embryonic/extraembryonic border (Figure 1C, 1H; Figure S1bG-S1bH). By the LB stage, strong *Bmp2* expression was found throughout the extraembryonic region, in both the extraembryonic visceral endoderm and mesoderm (Figure 1D, 1I). At HF stages, we observed *Bmp2* expression in cardiac crescent mesoderm and the overlying endoderm (Figure 1E, 1J). HF stage embryos also expressed *Bmp2* in extraembryonic mesoderm of the amnion and allantois (Figure 1E). *Bmp2* expression was not detected in ectodermal tissues at the DVE-HF stages.

Bmp2 Mutants Display Defects in Anterior Morphogenesis

Before initiating VE and epiblast-specific ablation of *Bmp2*, we characterized $Bmp2^{-/-}$ embryos (KO) to define distinct features that could be separately scored in KO and tissue-specific *Bmp2* mutants. In WT embryos, before the onset of turning (8-10 somite stage), the heart lies posterior/ventral to the head and both tissues are enclosed within the amnion (Figure 2A-2C). KO embryos, lacking *Bmp2* in all cell-types, arrest before turning and die by E10.5. They display a range of defects affecting formation of the amnion, head, and heart, which we sorted into four categories: 1) Open proamniotic canal, OPC; 2) Heart-outside the amnion, Ht-out; 3) Disorganized anterior, DAT; and 4) Unturned. An open proamniotic canal, a transient structure in WT neural plate stage embryos, persisted as an anterior horn-like extension as late as E10.5 in KO mutants with OPC (Figure 2D). In Ht-

out, the heart formed in the exocoelomic cavity, rather than within the amniotic cavity (Figure 2E). In DAT, the heart formed anterior/dorsal to the head instead of in its normal more posterior/ventral location (Figure 2F). The presence of contractile, beating tissue identified the location of the heart in living disorganized anterior embryos, while *in situ* detection of *Nkx2.5* and *Otx2* expression confirmed the identity of heart (Figure 3A-3B; 3E-3F) and head (Figure 3K-3L), respectively, in fixed embryos. Without exception, mutant embryos whose WT littermates had already completed turning, failed to turn. The unturned category includes genetically mutant embryos that did not show disorganized anterior, open proamniotic canal, or heart-outside amnion defects (Figure 2G).

The KO phenotype is highly variable during the somite stages (E8.5-E9.5), with failure to turn being the only consistent feature. A *Bmp2* KO embryo may present with one, two, three or, as depicted in Figure 2H, all four of the defects. We found that 63% (20/32) of KO embryos displayed disorganized anterior; 75% (27/36) open proamniotic canal, and 56% (14/25) heart-outside amnion (Table S2a). The 17% (8/47) not exhibiting disorganized anterior, open proamniotic canal or heart-outside amnion abnormalities still failed to turn (Table S2b).

The Disorganized Anterior Phenotype is Specific to VE-KO Embryos

To determine whether BMP2 expression in VE and epiblast derivatives regulates distinct or overlapping aspects of early post-implantation development, we used VE-(Kwon and Hadjantonakis, 2009) and epiblast-specific (Hayashi et al., 2002) Cre transgenes and a conditional *Bmp2* allele (Ma and Martin, 2005) to independently ablate *Bmp2* in each lineage. The *Ttr (*Transthyretin*)::Cre* transgene targets expression of Cre recombinase specifically to the VE layer of PS embryos. For inactivation in the VE lineage, we crossed $Bmp2^{flox/flox}$ females and $Bmp2^{\Delta 3/+;}$ *Ttr::Cre*/+ males to generate $Bmp2^{\Delta 3/flox}$; Ttr::Cre (VE-KO) embryos. In the $Bmp2^{flox}$ allele, loxP sites flank exon 3, which encodes the entire mature peptide. Consequently VE-KO embryos lack a functional gene ($Bmp2^{\Delta 3}$) in the VE, while continuing to express BMP2 in epiblast derivatives such as cardiac mesoderm, axial mesendoderm, and extraembryonic mesoderm of the amnion and yolk sac. We verified the VE-specificity of *Ttr::Cre* in WT and VE-KO embryos carrying the reporter allele *LacZR* (Soriano, 1999); (see Figure 5).

We examined 14 VE-KO embryos, eight at E8.5 and six at E9.5 (Table S2b). Similar to KO embryos, the VE-KO mutants arrested before turning, at the 8-10 somite stage. 75% (9/12) of the VE-KO embryos displayed the disorganized anterior phenotype; however, none showed open proamniotic canal or heart-outside amnion (Figure 2I; Table S2a). Thus, BMP2 expressed by epiblast derivatives is sufficient to rescue the amnion/heart defects found in KO embryos. On the other hand, proper positioning of the heart relative to the head requires BMP2 produced by the VE.

To inactivate *Bmp2* in epiblast-derivatives, $Bmp2^{flox/flox}$ females were mated to $Bmp2^{\Delta 3/+}$; *Sox2::Cre*/+ males to generate $Bmp2^{\Delta 3/flox}$; *Sox2::Cre* (EPI-KO) embryos. When transmitted by the male, the *Sox2::Cre* transgene directs Cre activity exclusively to the epiblast before gastrulation; therefore, *Bmp2* in the VE remains intact in EPI-KO embryos. We analyzed 20 EPI-KO embryos; eight at E8.5 and 12 at E9.5 (Table S2b). All of them failed to turn and arrested at midgestation. While 55% (6/11) of the EPI-KO embryos displayed open proamniotic canal and 42% (5/12) showed heart-outside amnion (Figure 2J), none presented the disorganized anterior phenotype (Table S2a). In addition, we observed a new phenotypic trait in 75% (9/12) of EPI-KO embryos at E9.5; posterior-specific delay (PSD; Table S2a, Table S2b, and Figure 2K). In embryos with posterior-specific delay, development of head structures (otic vesicle, eye and single branchial arch) was comparable to that in stage-matched WT littermates, yet the posterior region resembled that of the KO

mutant (Figure 2B-2C, 2H, 2K). Also, the medial heart tube did not undergo looping. These experiments indicate that the morphogenetic processes for properly positioning the head over the heart require BMP2 expressed in the VE lineage, whereas heart looping and inclusion of the heart within the amniotic membranes depend on BMP2 expression in epiblast-derived cell types. Closure of the proamniotic canal and completion of amnion formation also require BMP2 supplied by epiblast derivatives.

Cardiac and Neural Tissue Specification and Patterning Proceed Normally in the Absence of VE-expressed BMP2

Our analysis of KO embryos identified a previously unrecognized morphological defect in *Bmp2* mutants, a disorganized anterior region. Subsequent characterization of VE-KO and EPI-KO mutants revealed that the disorganized anterior phenotype specifically reflects loss of *Bmp2* expression in the VE. Two separate scenarios can be envisioned for the origin of the disorganized anterior defect. In one, misplacement of the heart relative to the head results from aberrant specification and/or patterning of cells in the ectoderm, mesoderm, and/or endoderm lineages during gastrulation. In the second, cell specification and patterning proceed normally, but tissues typically responsive to VE-supplied BMP2 fail to execute requisite morphogenetic cell behaviors, such as proliferation, migration and rearrangement. To distinguish between these possibilities, we performed whole mount *in situ* hybridization (WISH) to examine the expression of markers for the specification of cardiac mesoderm and neuroectoderm.

Prior to foregut invagination, during the EHF to early somite stages (~E8.0), myocardial progenitors derived from the first (FHF) and second (SHF) heart fields reside within the cardiac crescent region adjacent to the headfolds. EHF stage WT and KO embryos exhibited similar expression patterns for *Nkx2.5* (Figure 3A-3B), a marker for cardiac progenitors from both the FHF and SHF. At the 2-4 somite stage, when the disorganized anterior defect becomes morphologically recognizable, KO and VE-KO embryos expressed *Nkx2.5* and the SHF-specific transcript *Islet-1* within the cardiac crescent region, analogous to stage-matched controls (Figure 3C, 3C'-3D, 3D'; data not shown). By 20 somites, when WT littermates had completed heart looping, *Nkx2.5* staining showed only a small heart tube in KO embryos with the disorganized anterior trait (Figure 3E-3F'). These mutants also displayed lateral stripes of *Nkx2.5*+ cells, reminiscent of a partial cardia bifida (Figure 3F-3F'). These data indicate that specification of myocardial progenitors occurs in the total or VE-specific absence of BMP2; however formation of the linear heart tube remains incomplete in KO embryos.

In addition to perturbing A-P axis establishment, defective AVE formation and/or function can disrupt patterning of the anterior epiblast and subsequent steps in head development (Srinivas, 2006). To evaluate the proficiency of the AVE in VE-KO mutants we examined the expression of markers for development of the A-P axis and specification of neuroectoderm. E6.5 ES/MS stage VE-KO embryos displayed normal expression of the AVE markers *Cer1* and *Dkk1* and of the primitive streak marker *brachyury* (*T*, Figure 3G-3J). Thus as anticipated, loss of *Bmp2* in the VE did not perturb AVE formation or the delivery of the NODAL and WNT inhibitors required for the correct placement of the A-P axis.

Initial specification of the rostral neuroectoderm coincides with the elaboration of the A-P axis and depends on the AVE. Accordingly, mutants with impaired AVE function often exhibit forebrain truncations (Beddington and Robertson, 1999). To determine whether the irregular morphology of disorganized anterior KO and VE-KO mutants represents an anterior truncation, and potentially an AVE defect, or alternatively a misspecification of neural tissue, we performed WISH to a series of markers specific for distinct regions of the

neural tube. In WT embryos the forebrain markers *Foxg1* and *Six3* label the extreme anterior of the developing neural plate. Despite their radically different shape, disorganized anterior embryos expressed *Six3* in a restricted subset of anterior cells at the 6 somite (Figure 3M-3N) and 10 somite (Figure S3B, S3F, F') stages. Similarly, *Foxg1* is expressed in extreme anterior cells at the 8 somite stage in both WT and VE-KO embryos (Figure S3A, S3E, E'), thus ruling out a forebrain truncation. WT embryos at the early somite stage express *Otx2* in an anterior domain that extends to the midbrain/hindbrain boundary. VE-KO embryos exhibited a comparable distribution of *Otx2* at the early somite stages (Figure 3K-3L) and appropriately, *Otx2* extended more posteriorly than *Six3*. Disorganized anterior KO embryos expressed *En2*, a marker for the midbrain-hindbrain boundary, in a limited region of anterior ectoderm (Figure S3C, S3G, G'). Expression of *Egr2*, located in rhombomeres 3 and 5 of a WT hindbrain, was positioned in a discrete area posterior to the anterior tip in disorganized anterior KO mutants (Figure S3D, S3H, H'). Together these findings demonstrate that specification of forebrain, midbrain, and hindbrain cell populations persists in the absence of VE-expressed BMP2. Thus rather than misspecification or truncation, a morphogenetic mechanism must underlie the aberrant placement of head and heart in disorganized anterior VE-KO and KO embryos.

Disorganized Anterior Mutants Lack a Foregut Pocket

To elucidate the origin of the disorganized anterior phenotype, we determined the developmental stage at which morphological anomalies first emerge in VE-KO and KO embryos. VE-KO/KO mutants become morphologically distinguishable from WT embryos at the EHF stage, ~E7.75 (Figure S1a; Figure S4). In contrast to the rounded, distal tip in lateral views of WT embryos, the distal region of VE-KO embryos appeared flattened (Figure S4C-S4D; S4G-S4H). By the early somite stage, a subset of both KO and VE-KO embryos developed an anterior bulge, resembling the misplaced head observed in disorganized anterior mutants at the 8-10 somite stage (Figure 3C-3D, 3K-3N). While frontal views of early somite-stage WT embryos showed a single midline corresponding to the medial hinge point in the neural plate (Figure 4A), stage-matched KO and VE-KO embryos exhibited an ostensibly branching midline, suggesting the presence of multiple midlines across the neural plate (Figure 4B). While transverse sections verified a single medial hinge point and two lateral head folds in both the proximal and distal neural plate of WT embryos (Figure 4C, 4E), similar sections from KO embryos revealed uneven head folds proximally and ectopic hinge points distally (Figure 4D, 4F). KO and VE-KO *Bmp2* embryos expressed *Chordin*, *Shh*, and *brachyury* only medially (Figure 4G-4H; Figure S4K-S4L; data not shown), signifying a single notochord and eliminating multiple midlines as the source of ectopic neural folds in disorganized anterior mutants. Notably, although readily detectable in WT embryos, the foregut pocket was missing in all VE-KO embryos and in KO embryos exhibiting the disorganized anterior defect (Figure 4C-4D).

Scanning electron microscopy images more clearly depict the absence of the foregut pocket in disorganized anterior mutants (Figure 4I-4J). The frontal view of a WT early somite stage embryo shows the bilaminate midline extending from its posterior limit marked by the ciliated node to its anterior end which resides within the deep pocket formed by the involuting foregut (Figure 4I). In contrast, while the VE-KO embryo contains a ciliated node and a morphologically distinct midline, it lacks a detectable invagination at the anterior end of the midline (Figure 4J).

Absence of the foregut pocket consistently coincided with the appearance of ectopic neural folds and an elongated anterior axis, indicating that these three traits represent the defining features of the disorganized anterior phenotype. Moreover this finding implicates the formation of foregut invagination as an integral component of the morphogenetic process that positions head and heart.

Disorganized Anterior Mutants Undergo Specification and Early Patterning of Anterior Endoderm

At the LB-EHF stages, gut tube progenitors reside in a sheet of cells lining the ventral surface of the embryo (Zaret, 2008; Zorn and Wells, 2009). Initial patterning events within the endoderm layer specify anterior endoderm, which will contribute to the anterior intestinal portal (AIP or site of foregut invagination) and ultimately to all foregut derivatives (Franklin et al., 2008; Tremblay and Zaret, 2005). To determine whether disorganized anterior embryos contained appropriately specified and positioned anterior endoderm, we examined *Foxa2, Cer1*, *Chrd*, *Dkk1*, and *Gsc* expression in LB-to-EHF (E7.5-E8.0) embryos (Figure S4). WT and KO embryos displayed an analogous distribution of *Foxa2* and *Cer1* transcripts which mark the medial and lateral regions of foregut endoderm (Figure S4A-S4B; S4C, C'-S4F, F') (Ang et al., 1993; Kanai-Azuma et al., 2002; Shawlot et al., 1998). Similarly both WT and VE-KO embryos expressed *Dkk1* in a crescent-shaped region that included a segment of midline prechordal plate and adjacent prospective foregut endoderm (Figure S4G, G'-S4H, H') (Lewis and Tam, 2006). *Gsc* labels prechordal plate endoderm in EHF stage WT embryos; its domain of expression extends posteriorly from *Dkk1* but resides anterior to *Chrd* in the anterior head process. EHF stage VE-KO embryos stained comparably to WT with *Gsc* and *Chrd* (Figure S4I, I'-S4L, L'). Since *Dkk1 and Gsc* labeled endoderm cells will contribute, respectively, to ventral and dorsal foregut (Lewis et al., 2007), these data indicate that VE-KO embryos appropriately patterned anterior endoderm. Thus the lack of foregut invagination in disorganized anterior mutant embryos does not reflect an absence of endoderm specification and early patterning.

The Definitive Endoderm Layer Includes *Bmp2*$^{-/-}$ VE plus *Bmp2*$^{+/+}$ epiblast-derived Cells

The absence of the foregut invagination in VE-KO and disorganized anterior KO mutants suggested that *Bmp2* expression in the VE has a critical role in foregut morphogenesis. VE derivatives not only comprise the entire endodermal layer of the visceral yolk sac in the HF stage embryo, but also populate the developing sheet of embryonic endoderm cells (Kwon et al., 2008; Nowotschin and Hadjantonakis, 2010). To ask whether VE-expressed BMP2 is required for the persistence of VE derivatives in anterior endoderm, we examined the distribution of VE descendants in the anterior midline before and after foregut pocket formation using the *Ttr::Cre*/+ transgene and the *LacZR*/+ Cre-reporter allele. Wild-type *Ttr::Cre*/+; *LacZR*/+ embryos at E 7.5-E 8.5 contain VE derivatives in both extraembryonic and embryonic cell layers. Prior to foregut invagination, the latter population of VE descendants resided in a speckled pattern across the anterior midline of WT embryos (Figure 5A-5A"). In VE-KO embryos the LacZ positive VE cells adopted a similar distribution (Figure 5D-5D"). At the early and 8-10 somite stages, following foregut invagination, wild-type *Ttr::Cre*/+; *LacZR*/+ embryos displayed VE derivatives throughout the internalized, primitive gut tube (Figure 5B-5B", 5C-5C"; (Kwon and Hadjantonakis, 2009; Kwon et al., 2008). In contrast, we detected no internalized LacZ-expressing VE cells in early and 8-10 somite stage *Ttr::Cre*/+; *LacZR*/+ VE-KO and disorganized anterior KO embryos, despite their continued presence in the embryonic endoderm layer (Figure 5E-5E", 5F-5F"). Therefore, in the absence of VE-expressed BMP2, VE-descendants remain competent to integrate with ingressing epiblast-derived cells to generate the definitive (or primitive) gut endoderm layer. Yet, neither anterior endoderm cells derived from the *Bmp2*$^{-/-}$ VE nor the *Bmp2*$^{flox/flox}$ epiblast were able to participate in foregut invagination. These findings combined with the marker analyses indicate that the primary function of VE-expressed BMP2 is to activate the signaling pathways that direct the morphogenetic processes required for both foregut invagination and positioning of head and heart.

Anterior Neural Folds Abnormally Expand Outwards in Disorganized Anterior Mutants

Since the characteristic features of disorganized anterior *Bmp2* mutants indicated that positioning of head and heart is mechanistically linked to formation of the foregut invagination, we investigated the arrangement of cells comprising the ectopic head folds in VE-KO embryos at the level of the missing foregut pocket using confocal microscopy to examine SOX2 and E-cadherin (Ecad) expression (Figure 6A-6F). Antibodies to SOX2 and Ecad stained, respectively, neuroectoderm and endoderm, while mesoderm cells were positive for DAPI but negative for both SOX2 and Ecad. 3D reconstructions of embryos viewed from a frontal perspective located SOX2 positive neural folds adjacent to the midline in WT embryos (Figure 6A, 6C). In VE-KO embryos, SOX2 expressing ectodermal cells failed to organize around a distinct midline (Figure 6B, 6D). In both WT and VE-KO, a surface layer of Ecad-positive endoderm cells overlaid the SOX2 stained ectoderm (Figure 6C-6D). Single XY sections of the frontal views defined more clearly the topographical differences between WT and VE-KO embryos (Figure 6E-6F). In the WT embryo such sections revealed an endoderm-lined crescent-shaped cavity at the level of the foregut invagination. The absence of anterior SOX2-positive neurectodermal folds in the XY slices indicated that the involuting foregut shifted the anterior midline out of a plane of section containing the distal midline and node (Figure 6A', 6E). In contrast, equivalent XY sections of the VE-KO embryo did not contain a distinct, well-formed endoderm-lined cavity; furthermore, such sections included SOX2-labeled neurectodermal folds but not the distal midline and node (Figure 6B', 6F). These observations indicate that in contrast to neural folds in WT embryos which were shifted inwards during formation of the foregut pocket (Figure 6A, 6C, 6E), the neural folds in early somite-stage VE-KO embryos expanded outward to form the anterior bulge observed in head fold stage mutants (Figure 6B, 6D, 6F).

DISCUSSION

Our studies provide new insight into the spatial and temporal organization of the signaling pathways that initiate ventral morphogenesis, a fundamental but poorly understood developmental process that, in amniotes, internalizes the gut tube, closes the ventral body wall, and encases the embryo in extraembryonic membranes (Brewer and Williams, 2004; Sadler, 2010). We find that BMP2 from the VE regulates key aspects of early ventral folding morphogenesis, including formation of foregut invagination and proper placement of head and heart. Notably, our examination of temporal and spatial patterns of transcription identifies a discrete region of the AVE as the primary source of BMP2 at the onset of gastrulation and during the initiation of ventral folding. The domain of *Bmp2* expression at the ES stage resides within the region of the VE that was found in recent genetic fate mapping experiments to contain all progeny of *Lefty1*+ cells in the DVE at E5.25 (Takaoka et al., 2011). Intriguingly, the E5.25 *Lefty1*+-DVE derivatives occupy a distinct anterior/lateral region of the VE from distal VE cells first expressing *Lefty1* and *Cer*1 after E5.5; the latter cell population forms what is conventionally defined as the AVE, based on *Hex* expression at E6.5 (Takaoka et al., 2011). To further characterize the BMP2-expressing subset of anterior, proximal VE cells, it will be important to determine whether it derives directly from the *Lefty1*+-DVE cells at E5.25 and whether signals from more distal AVE cells regulate its expression of BMP2, as suggested by Stuckey et al (Stuckey et al., 2011).

VE-expressed BMP2 Signals to Receptors on Epiblast-derived Cells

Of the three type I receptors responsive to BMP2, only *Bmpr1a* (*Alk3*) is expressed ubiquitously at pre-streak and early gastrulation stages (Mishina et al., 1995; Roelen et al., 1994); *Acvr1* (Activin A receptor, type I or *Alk2*) expression is restricted to the VE (Gu et al., 1999) and *Bmpr1b* (*Alk6*) transcription has not been reported before E9.5 (Dewulf et al., 1995). Therefore the disorganized anterior phenotype likely results from loss of BMP2

signaling to ACVR1 and/or BMPR1A. Neither *Acvr1* nor *Bmpr1a* KO embryos recapitulate the disorganized anterior or other *Bmp2* mutant phenotypes; both receptor KOs arrest earlier and display more severe defects than *Bmp2* KO embryos. *Acvr1* null embryos exhibit irregular VE morphology, limited mesoderm formation, and developmental arrest at early gastrulation (Gu et al., 1999). *Bmpr1a* mutants arrest before gastrulation and lack all mesoderm (Mishina et al., 1995), abnormalities resembling those observed in most *Bmp4* KO embryos (Winnier et al., 1995). Thus the *Bmpr1a* KO phenotype primarily reflects loss of BMP4 signaling following implantation and obscures a potential later role for BMPR1A in BMP2 signaling. While deletion of *Bmpr1a* in all epiblast cells largely recapitulates the *Bmp4* null phenotype (Di-Gregorio et al., 2007), mosaic deletion of *Bmpr1a* within the epiblast permits sufficient signaling to rescue early defects and allow mutant embryos to gastrulate (Davis et al., 2004). Pertinently, embryos with a mosaic loss of *Bmpr1a* in epiblast-derived cells display ectopic neural folds, lack the foregut invagination, and exhibit an abnormally elongated anterior region, key features of the disorganized anterior phenotype described here for *Bmp2* VE-KO embryos. These data are strong evidence that BMP2 expressed in the VE signals through its cognate receptor, BMPR1a, in epiblast-derived cells to regulate the onset of ventral morphogenesis. Moreover, studies on embryos deficient for *Smad5* concur with this proposed pathway. At the pre and early streak stages *Smad5* is transcribed in the epiblast but not in extraembryonic ectoderm and VE; similar to *Bmp2* VE-KO embryos, late headfold-to-early somite stage $Smad5^{-/-}$ mutants lack the foregut invagination and contain ectopic neural folds (Chang et al., 1999).

VE-secreted factors active in organizing and patterning the early gastrula function as inhibitors of the WNT (DKK1) or NODAL (CERL, LEFTY1) pathways. Conversely, we show that BMP2 expressed by the VE/AVE acts on epiblast derivatives to activate a morphogenetic program.

Head Morphogenesis Requires VE-expressed BMP2

In Xenopus, chick, and zebrafish, neural induction requires inhibition of BMP signaling (Gaulden and Reiter, 2008). Similarly in mouse, epiblast cells lacking *Bmpr1a* prematurely initiate neural differentiation, indicating that BMP signaling maintains pluripotency by blocking neural induction (Di-Gregorio et al., 2007). Correspondingly, expression of the BMP antagonists Chordin and Noggin initiates concurrently with neural induction at the MS-LS stages; transcription of *Chordin* (*Chrd*) and *Noggin* (*Nog*) begins within the anterior primitive streak/node and continues in the axial mesendoderm up to the caudal boundary of the prechordal plate (Anderson et al., 2002; Bachiller et al., 2000). $Chrd^{-/-}$; $Nog^{-/-}$ mutant embryos exhibit a severely reduced forebrain but relatively normal midbrain and hindbrain at E12.5 (Bachiller et al., 2000). Thus the elevated levels of BMP activity generated in the absence of Chordin and Noggin specifically inhibit forebrain development. If VE-BMP2 is the main source of this elevated activity, then VE-KO embryos would be expected to have preferentially expanded or prematurely differentiated forebrain. Based on the expression of neural markers in disorganized anterior mutants, specification and patterning of forebrain occurs appropriately relative to midbrain and hindbrain, suggesting that Chordin and Noggin do not normally regulate VE-BMP2. Consistent with this interpretation, the domains of *Bmp2* expression in the VE do not overlap with those of *Chordin* and *Noggin*. *Bmp2* is initially expressed throughout the EmVE before the onset of *Chordin* and *Noggin* expression; subsequently, at the ES-MS stages, *Bmp2* resides in the AVE, distinctly anterior to *Chordin* and *Noggin*.

The ectopic neural folds observed in the elongated anterior region of VE-KO embryos with the disorganized anterior defect may arise from elevated levels of proliferation in neuroectoderm or from conversion of surface ectoderm into neuroectoderm, as proposed by Davis et al. (2004) for the multiple neural folds in mosaic EPI-*Bmpr1a* KO embryos.

However, WISH to neural markers did not detect enlarged regions of expression in VE-KO mutants compared to WT embryos (Figures 3 and S3). We also did not observe a noticeable loss of surface ectoderm (Figure 4E-4F). An alternative explanation for the aberrantly elongated anterior region is that the neuroectoderm collapses into extra neural folds in the absence of VE-BMP2-activated ventral folding morphogenesis.

VE-expressed BMP2 Links Foregut Invagination and Head Morphogenesis

Specification, formation, and early patterning of anterior endoderm proceed appropriately in disorganized anterior VE-KO embryos. Consequently their lack of a foregut pocket indicates that VE-expressed BMP2 promotes invagination of foregut endoderm by regulating morphogenetic events rather than cell differentiation. Between the EHF and early somite stages foregut invagination initiates internalization of the gut tube, marking the onset of ventral folding. Tracking endoderm cells in cultured embryos demonstrated a rostral-caudal repositioning of endoderm cells along the midline as the anterior endoderm transitions from a convex external layer into a concave internal foregut pocket (Franklin et al., 2008). During this same time period, neuroectoderm undergoes a rostral-caudal reorganization to form the headfolds and to position them anterior to cardiac mesoderm. Although foregut invagination proceeds concomitantly with head and heart repositioning, the extent to which these events are mechanistically connected is unknown. The discovery that VE-expressed BMP2 regulates both formation of the foregut pocket and positioning of head and heart now provides a framework for building and assessing models for the cellular mechanisms underlying anterior and ventral folding morphogenesis.

The top row in Figure 7 diagrams predicted movements of the embryonic endoderm, cardiac mesoderm, and neuroectoderm layers during foregut invagination and head fold formation in a WT embryo (Video abstract). At the EHF stage the developing heart resides anterior to the nascent head folds(DeRuiter et al., 1992). Subsequently, with the concomitant invagination of foregut and expansion of neuroectoderm, the heart shifts to a posterior, ventral position relative to the head folds (Dunwoodie et al., 1998). In the absence of VE-expressed BMP2, foregut endoderm fails to invaginate and the heart remains anterior to the growing head folds (bottom row, Figure 7), generating the disorganized anterior phenotype.

AVE cells expressing BMP2 reside in a region where the extraembryonic endoderm, mesoderm, and ectoderm layers of the yolk sac and amnion converge with the definitive endoderm, cardiac mesoderm, and neuroectoderm layers of the embryo (Figure 7 top row). Thus AVE-produced BMP2 could potentially signal to BMPR1A on epiblast derivatives in any of these adjoining cell layers; (all cell types in the layers portrayed in Figure 7 are epiblast-derived, except for the VE). Likely target tissues for anterior morphogenesis include epiblast-derived gut endoderm cells adjacent to EmVE derived cells, neuroectoderm, and cardiac mesoderm. A key issue for future investigation is whether VE-expressed BMP2 coordinates foregut invagination and head fold morphogenesis by signaling to one or more distinct cell layers; i.e. to gut endoderm and/or neuroectoderm and cardiac mesoderm. A related question concerns when VE-BMP2 signaling is required; the disorganized anterior phenotype may reflect loss of *BMP2* from the EmVE prior to gastrulation as well as its later absence from the AVE.

Anterior Ventral Morphogenesis and Positioning of the Primitive Heart Tube

The AIP, an arc of thickened endoderm spanning the midline and overlying splanchnic mesoderm, marks the site at which foregut invagination initiates; its appearance at the LB/EHF stage denotes the onset of ventral folding morphogenesis. Histological analyses (DeRuiter et al., 1992) and short-term cell labeling studies (Tam et al., 2004; Tremblay and Zaret, 2005) indicate that the midline and lateral edges of primitive gut endoderm fold

inward and fuse to form the anterior gut tube. Concomitantly, lateral-to-ventral movements of bilateral precardiac splanchnic mesoderm and of body wall mesoderm and ectoderm result in a linear heart tube and ventral closure, respectively. Embryos with defective lateral-to-ventral movements of precardiac mesoderm lack a linear heart tube and develop two primitive hearts or cardia bifida.

Targeted mutations in a variety of genes result in cardia bifida, including the transcription factor *Gata4* (Kuo et al., 1997; Molkentin et al., 1997), the vesicular trafficking protein *Hgs/Hrs* (HGF-regulated tyrosine kinase substrate) (Komada and Soriano, 1999), *Furin*, a proprotein convertase (Constam and Robertson, 2000), and *Flrt3* (fibronectin leucine rich transmembrane protein 3) (Maretto et al., 2008). Defects in foregut development invariably accompany cardia bifida in each of these mutants. This finding suggests that a single morphogenetic process, involving interplay between endoderm and lateral mesoderm, drives formation of both the anterior gut and the linear heart tube during the initial stages of ventral folding. In this scenario, the generation of a single linear heart tube depends on the formation of foregut invagination. However, the *Bmp2* VE-KO embryos challenge this view; they lack the foregut invagination, yet still display a medial heart tube.

Anterior ventral morphogenesis achieves formation and placement of the foregut and medial heart tubes through rostral-to-caudal and lateral-to-ventral tissue folding. Rostral-to-caudal folding positions the heart posterior to the head folds and generates the foregut pocket; lateral-to-ventral folding fuses the bilateral heart primordia and closes the gut tube at the ventral midline. In the absence of VE-expressed BMP2, anterior endoderm fails to undergo both rostral-to-caudal and ventral-to-lateral folding, resulting in the lack of the foregut pocket and a closed gut tube. The presence of a single heart tube in VE-KO embryos indicates that the morphogenetic process mediating the lateral-to-ventral movement of anterior splanchnic mesoderm proceeds independently of anterior gut tube folding. Conversely, the disorganized anterior phenotype of *Bmp2* VE-KO mutants argues that a single morphogenetic process achieves both formation of foregut invagination and correct rostral-to-caudal positioning of head and heart. Distinct differences in the foregut and heart defects displayed by the cardia bifida mouse mutants support this model. Both the *Gata4* (Kuo et al., 1997; Molkentin et al., 1997) and *Hgs/Hrs* (Komada and Soriano, 1999) KOs completely lack foregut invagination and the bilateral heart primordia reside anterior to the headfolds. In the *Furin* (Roebroek et al., 1998) and *Flrt3* (Maretto et al., 2008) mutants, however, the foregut pocket forms but does not close ventrally. Consistent with a single morphogenetic process driving foregut invagination and rostral-caudal positioning of head and heart, the bilateral heart primordia appropriately reside posterior to the headfolds.

EXPERIMENTAL PROCEDURES

Immunohistochemistry

Embryos dissected in cold DMEM/F12 plus 5% newborn calf serum were fixed for 10-20 min, then blocked and permeabilized in PBSMT (PBS containing 2% non-fat dry milk powder, Bio-Rad) and 0.5 % Triton X-100, 3x one hr each. Embryos were incubated overnight at 4°C with antibodies diluted in PBSMT: rabbit anti-SOX2 (1:1000 Chemicon), rat anti-E-Cad (1:500, Sigma). After washing in freshly prepared PBSMT at 4°C, with three changes over ≥ 3 hrs, embryos were incubated with secondary antibodies at 1:250 and DAPI at 1:1000 for 2 hrs at room temperature or overnight at 4°C. Before imaging, embryos were washed 3x in PBSMT at 4°C for ≥ 3 hrs and rinsed 3x in PBS at room temperature.

Whole Mount *In Situ* Hybridization

Whole mount *in situ* hybridization was performed as described (Belo et al., 1997) and RNA probes were prepared according to (Nagy et al., 2003). For two-color *in situ* hybridization; the blocking, antibody incubation, and color development steps were performed to first detect the fluorescein-labeled RNA probe. Next the embryos were fixed in 4% PFA and the antibody inactivated by washing twice for 20 min in 100 mM glycine—HCl, pH 2.2. All three steps were then repeated to detect the digoxigenin-labeled RNA probe. Staining for β-galactosidase activity was performed by established methods (Nagy et al., 2003).

Scanning Electron Microscopy

Embryos dissected in cold PBS were fixed overnight at 4°C in 2.5% glutaraldehyde, washed 3X -15 min each-in PBS, and dehydrated in a graded series of ethanol. After drying in a Denton JCP-1 Critical Point Dryer, the samples were coated with Gold/Palladium in a Denton Vacuum Desk 1V Sputter Coater. The samples were viewed with a Zeiss Supra 25 Field Emission Scanning Electron Microscope.

Genotyping

E6.5-E7.5 whole embryos and E8.5-9.5 yolk sac fragments were added to 100ul 50mM NaOH, boiled 20 min, and vortexed. The samples were neutralized with 8ul 1M TRIS pH8, centrifuged at 12K for six min; PCR reactions were run with 1ul. See Supplemental Information for primer sequences.

All animal experimentation was approved by the SKI IACUC; we followed IACUC policies for minimizing distress and pain in all procedures performed on mice and embryos.

Supplementary Material

Refer to Web version on PubMed Central for supplementary material.

Acknowledgments

We thank JF Martin, AK Hadjantonakis, and TA Rodriguez for generously providing, respectively, *Bmp2*$^{flox/+}$, *Ttr::Cre*, and *Hex-GFP* mice; the MSKCC Mouse Genetics Core for blastocyst injections; and the MSKCC Molecular Cytology Core for guidance on confocal microscopy. We are grateful to KV Anderson, AK Hadjantonakis, F Lupu, and L Selleri for valuable discussions; to A Foley and E Freed for insightful comments on the manuscript, and A Poon for her work on the Video abstract. This research was supported by NIH RO1 GM58726. The authors declare no competing financial interests related to this work.

References

Anderson RM, Lawrence AR, Stottmann RW, Bachiller D, Klingensmith J. Chordin and noggin promote organizing centers of forebrain development in the mouse. Development. 2002; 129:4975–4987. [PubMed: 12397106]

Ang SL, Wierda A, Wong D, Stevens KA, Cascio S, Rossant J, Zaret KS. The formation and maintenance of the definitive endoderm lineage in the mouse: involvement of HNF3/forkhead proteins. Development. 1993; 119:1301–1315. [PubMed: 8306889]

Arnold SJ, Robertson EJ. Making a commitment: cell lineage allocation and axis patterning in the early mouse embryo. Nat Rev Mol Cell Biol. 2009; 10:91–103. [PubMed: 19129791]

Bachiller D, Klingensmith J, Kemp C, Belo JA, Anderson RM, May SR, McMahon JA, McMahon AP, Harland RM, Rossant J, et al. The organizer factors Chordin and Noggin are required for mouse forebrain development. Nature. 2000; 403:658–661. [PubMed: 10688202]

Beddington RS, Robertson EJ. Axis development and early asymmetry in mammals. Cell. 1999; 96:195–209. [PubMed: 9988215]

Belo JA, Bouwmeester T, Leyns L, Kertesz N, Gallo M, Follettie M, De Robertis EM. Cerberus-like is a secreted factor with neutralizing activity expressed in the anterior primitive endoderm of the mouse gastrula. Mech Dev. 1997; 68:45–57. [PubMed: 9431803]

Biben C, Stanley E, Fabri L, Kotecha S, Rhinn M, Drinkwater C, Lah M, Wang CC, Nash A, Hilton D, et al. Murine cerberus homologue mCer-1: a candidate anterior patterning molecule. Dev Biol. 1998; 194:135–151. [PubMed: 9501024]

Brewer S, Williams T. Finally, a sense of closure? Animal models of human ventral body wall defects. Bioessays. 2004; 26:1307–1321. [PubMed: 15551266]

Chang H, Huylebroeck D, Verschueren K, Guo Q, Matzuk MM, Zwijsen A. Smad5 knockout mice die at mid-gestation due to multiple embryonic and extraembryonic defects. Development. 1999; 126:1631–1642. [PubMed: 10079226]

Constam DB, Robertson EJ. Tissue-specific requirements for the proprotein convertase furin/SPC1 during embryonic turning and heart looping. Development. 2000; 127:245–254. [PubMed: 10603343]

Coucouvanis E, Martin GR. BMP signaling plays a role in visceral endoderm differentiation and cavitation in the early mouse embryo. Development. 1999; 126:535–546. [PubMed: 9876182]

Davis S, Miura S, Hill C, Mishina Y, Klingensmith J. BMP receptor IA is required in the mammalian embryo for endodermal morphogenesis and ectodermal patterning. Dev Biol. 2004; 270:47–63. [PubMed: 15136140]

DeRuiter MC, Poelmann RE, VanderPlas-de Vries I, Mentink MM, Gittenberger-de Groot AC. The development of the myocardium and endocardium in mouse embryos. Fusion of two heart tubes? Anat Embryol (Berl). 1992; 185:461–473. [PubMed: 1567022]

Dewulf N, Verschueren K, Lonnoy O, Moren A, Grimsby S, Vande Spiegle K, Miyazono K, Huylebroeck D, Ten Dijke P. Distinct spatial and temporal expression patterns of two type I receptors for bone morphogenetic proteins during mouse embryogenesis. Endocrinology. 1995; 136:2652–2663. [PubMed: 7750489]

Di-Gregorio A, Sancho M, Stuckey DW, Crompton LA, Godwin J, Mishina Y, Rodriguez TA. BMP signalling inhibits premature neural differentiation in the mouse embryo. Development. 2007; 134:3359–3369. [PubMed: 17699604]

Dunwoodie SL, Rodriguez TA, Beddington RS. Msg1 and Mrg1, founding members of a gene family, show distinct patterns of gene expression during mouse embryogenesis. Mech Dev. 1998; 72:27–40. [PubMed: 9533950]

Franklin V, Khoo PL, Bildsoe H, Wong N, Lewis S, Tam PP. Regionalisation of the endoderm progenitors and morphogenesis of the gut portals of the mouse embryo. Mech Dev. 2008; 125:587–600. [PubMed: 18486455]

Fujiwara T, Dehart DB, Sulik KK, Hogan BL. Distinct requirements for extra-embryonic and embryonic bone morphogenetic protein 4 in the formation of the node and primitive streak and coordination of left-right asymmetry in the mouse. Development. 2002; 129:4685–4696. [PubMed: 12361961]

Gaulden J, Reiter JF. Neur-ons and neur-offs: regulators of neural induction in vertebrate embryos and embryonic stem cells. Hum Mol Genet. 2008; 17:R60–66. [PubMed: 18632699]

Gu Z, Reynolds EM, Song J, Lei H, Feijen A, Yu L, He W, MacLaughlin DT, van den Eijnden-van Raaij J, Donahoe PK, et al. The type I serine/threonine kinase receptor ActRIA (ALK2) is required for gastrulation of the mouse embryo. Development. 1999; 126:2551–2561. [PubMed: 10226013]

Hayashi S, Lewis P, Pevny L, McMahon AP. Efficient gene modulation in mouse epiblast using a Sox2Cre transgenic mouse strain. Mech Dev. 2002; 119(Suppl 1):S97–S101. [PubMed: 14516668]

Kanai-Azuma M, Kanai Y, Gad JM, Tajima Y, Taya C, Kurohmaru M, Sanai Y, Yonekawa H, Yazaki K, Tam PP, et al. Depletion of definitive gut endoderm in Sox17-null mutant mice. Development. 2002; 129:2367–2379. [PubMed: 11973269]

Kanzler B, Foreman RK, Labosky PA, Mallo M. BMP signaling is essential for development of skeletogenic and neurogenic cranial neural crest. Development. 2000; 127:1095–1104. [PubMed: 10662648]

Kimura-Yoshida C, Nakano H, Okamura D, Nakao K, Yonemura S, Belo JA, Aizawa S, Matsui Y, Matsuo I. Canonical Wnt signaling and its antagonist regulate anterior-posterior axis polarization

by guiding cell migration in mouse visceral endoderm. Dev Cell. 2005; 9:639–650. [PubMed: 16256739]

Komada M, Soriano P. Hrs, a FYVE finger protein localized to early endosomes, is implicated in vesicular traffic and required for ventral folding morphogenesis. Genes Dev. 1999; 13:1475–1485. [PubMed: 10364163]

Kuo CT, Morrisey EE, Anandappa R, Sigrist K, Lu MM, Parmacek MS, Soudais C, Leiden JM. GATA4 transcription factor is required for ventral morphogenesis and heart tube formation. Genes Dev. 1997; 11:1048–1060. [PubMed: 9136932]

Kwon GS, Hadjantonakis AK. Transthyretin mouse transgenes direct RFP expression or Cre-mediated recombination throughout the visceral endoderm. Genesis. 2009; 47:447–455. [PubMed: 19415627]

Kwon GS, Viotti M, Hadjantonakis AK. The endoderm of the mouse embryo arises by dynamic widespread intercalation of embryonic and extraembryonic lineages. Dev Cell. 2008; 15:509–520. [PubMed: 18854136]

Lawson KA, Pedersen RA. Cell fate, morphogenetic movement and population kinetics of embryonic endoderm at the time of germ layer formation in the mouse. Development. 1987; 101:627–652. [PubMed: 3502998]

Lewis SL, Khoo PL, Andrea De Young R, Bildsoe H, Wakamiya M, Behringer RR, Mukhopadhyay M, Westphal H, Tam PP. Genetic interaction of Gsc and Dkk1 in head morphogenesis of the mouse. Mech Dev. 2007; 124:157–165. [PubMed: 17127040]

Lewis SL, Tam PP. Definitive endoderm of the mouse embryo: formation, cell fates, and morphogenetic function. Dev Dyn. 2006; 235:2315–2329. [PubMed: 16752393]

Ma L, Martin JF. Generation of a Bmp2 conditional null allele. Genesis. 2005; 42:203–206. [PubMed: 15986484]

Mao J, McKean DM, Warrier S, Corbin JG, Niswander L, Zohn IE. The iron exporter ferroportin 1 is essential for development of the mouse embryo, forebrain patterning and neural tube closure. Development. 2010; 137:3079–3088. [PubMed: 20702562]

Maretto S, Muller PS, Aricescu AR, Cho KW, Bikoff EK, Robertson EJ. Ventral closure, headfold fusion and definitive endoderm migration defects in mouse embryos lacking the fibronectin leucine-rich transmembrane protein FLRT3. Dev Biol. 2008; 318:184–193. [PubMed: 18448090]

Mesnard D, Guzman-Ayala M, Constam DB. Nodal specifies embryonic visceral endoderm and sustains pluripotent cells in the epiblast before overt axial patterning. Development. 2006; 133:2497–2505. [PubMed: 16728477]

Mishina Y, Suzuki A, Ueno N, Behringer RR. Bmpr encodes a type I bone morphogenetic protein receptor that is essential for gastrulation during mouse embryogenesis. Genes Dev. 1995; 9:3027–3037. [PubMed: 8543149]

Molkentin JD, Lin Q, Duncan SA, Olson EN. Requirement of the transcription factor GATA4 for heart tube formation and ventral morphogenesis. Genes Dev. 1997; 11:1061–1072. [PubMed: 9136933]

Nagy, A.; Gertsenstein, M.; Vintersten, K.; Behringer, RR. Manipulating the Mouse Embryo. third edn. Cold Spring Harbor Laboratory Press; 2003.

Nowotschin S, Hadjantonakis AK. Cellular dynamics in the early mouse embryo: from axis formation to gastrulation. Curr Opin Genet Dev. 2010; 20:420–427. [PubMed: 20566281]

Perea-Gomez A, Shawlot W, Sasaki H, Behringer RR, Ang S. HNF3beta and Lim1 interact in the visceral endoderm to regulate primitive streak formation and anterior-posterior polarity in the mouse embryo. Development. 1999; 126:4499–4511. [PubMed: 10498685]

Perea-Gomez A, Vella FD, Shawlot W, Oulad-Abdelghani M, Chazaud C, Meno C, Pfister V, Chen L, Robertson E, Hamada H, et al. Nodal antagonists in the anterior visceral endoderm prevent the formation of multiple primitive streaks. Dev Cell. 2002; 3:745–756. [PubMed: 12431380]

Rhinn M, Dierich A, Shawlot W, Behringer RR, Le Meur M, Ang SL. Sequential roles for Otx2 in visceral endoderm and neuroectoderm for forebrain and midbrain induction and specification. Development. 1998; 125:845–856. [PubMed: 9449667]

Rivera-Perez JA, Mager J, Magnuson T. Dynamic morphogenetic events characterize the mouse visceral endoderm. Dev Biol. 2003; 261:470–487. [PubMed: 14499654]

Rodriguez TA, Srinivas S, Clements MP, Smith JC, Beddington RS. Induction and migration of the anterior visceral endoderm is regulated by the extra-embryonic ectoderm. Development. 2005; 132:2513–2520. [PubMed: 15857911]

Roebroek AJ, Umans L, Pauli IG, Robertson EJ, van Leuven F, Van de Ven WJ, Constam DB. Failure of ventral closure and axial rotation in embryos lacking the proprotein convertase Furin. Development. 1998; 125:4863–4876. [PubMed: 9811571]

Roelen BA, Lin HY, Knezevic V, Freund E, Mummery CL. Expression of TGF-beta s and their receptors during implantation and organogenesis of the mouse embryo. Dev Biol. 1994; 166:716–728. [PubMed: 7813789]

Sadler TW. The embryologic origin of ventral body wall defects. Semin Pediatr Surg. 2010; 19:209–214. [PubMed: 20610194]

Shawlot W, Deng JM, Behringer RR. Expression of the mouse cerberus-related gene, Cerr1, suggests a role in anterior neural induction and somitogenesis. Proc Natl Acad Sci U S A. 1998; 95:6198–6203. [PubMed: 9600941]

Soriano P. Generalized lacZ expression with the ROSA26 Cre reporter strain. Nat Genet. 1999; 21:70–71. [PubMed: 9916792]

Srinivas S. The anterior visceral endoderm-turning heads. Genesis. 2006; 44:565–572. [PubMed: 17078044]

Srinivas S, Rodriguez T, Clements M, Smith JC, Beddington RS. Active cell migration drives the unilateral movements of the anterior visceral endoderm. Development. 2004; 131:1157–1164. [PubMed: 14973277]

Stuckey DW, Di Gregorio A, Clements M, Rodriguez TA. Correct patterning of the primitive streak requires the anterior visceral endoderm. PLoS One. 2011; 6:e17620. [PubMed: 21445260]

Takaoka K, Yamamoto M, Hamada H. Origin and role of distal visceral endoderm, a group of cells that determines anterior-posterior polarity of the mouse embryo. Nat Cell Biol. 2011; 13:743–752. [PubMed: 21623358]

Tam PP, Khoo PL, Wong N, Tsang TE, Behringer RR. Regionalization of cell fates and cell movement in the endoderm of the mouse gastrula and the impact of loss of Lhx1(Lim1) function. Dev Biol. 2004; 274:171–187. [PubMed: 15355796]

Thomas P, Beddington R. Anterior primitive endoderm may be responsible for patterning the anterior neural plate in the mouse embryo. Curr Biol. 1996; 6:1487–1496. [PubMed: 8939602]

Tremblay KD, Zaret KS. Distinct populations of endoderm cells converge to generate the embryonic liver bud and ventral foregut tissues. Dev Biol. 2005; 280:87–99. [PubMed: 15766750]

Winnier G, Blessing M, Labosky PA, Hogan BL. Bone morphogenetic protein-4 is required for mesoderm formation and patterning in the mouse. Genes Dev. 1995; 9:2105–2116. [PubMed: 7657163]

Yamamoto M, Beppu H, Takaoka K, Meno C, Li E, Miyazono K, Hamada H. Antagonism between Smad1 and Smad2 signaling determines the site of distal visceral endoderm formation in the mouse embryo. J Cell Biol. 2009; 184:323–334. [PubMed: 19153222]

Ying Y, Zhao GQ. Cooperation of endoderm-derived BMP2 and extraembryonic ectoderm-derived BMP4 in primordial germ cell generation in the mouse. Dev Biol. 2001; 232:484–492. [PubMed: 11401407]

Zaret KS. Genetic programming of liver and pancreas progenitors: lessons for stem-cell differentiation. Nat Rev Genet. 2008; 9:329–340. [PubMed: 18398419]

Zhang H, Bradley A. Mice deficient for BMP2 are nonviable and have defects in amnion/chorion and cardiac development. Development. 1996; 122:2977–2986. [PubMed: 8898212]

Zorn AM, Wells JM. Vertebrate endoderm development and organ formation. Annu Rev Cell Dev Biol. 2009; 25:221–251. [PubMed: 19575677]

HIGHLIGHTS

- Proximal anterior visceral endoderm (AVE) expresses BMP2 at onset of gastrulation
- AVE- and epiblast-derived BMP2 perform separate roles during gastrulation
- AVE-derived BMP2 signals to epiblast to initiate ventral folding morphogenesis
- Foregut invagination and positioning of head and heart require AVE-derived BMP2

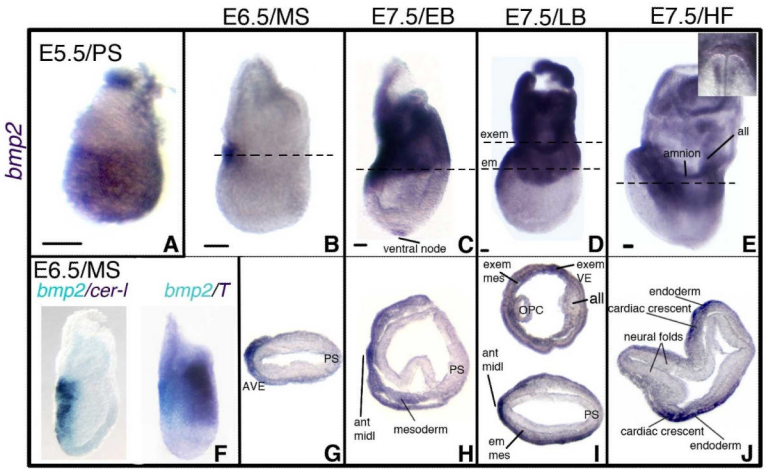

Figure 1. Pre-Streak to Head Fold Stage Embryos Express *Bmp2* in the AVE

(A-J) *Bmp2* expression at E5.5/Pre-streak, (PS) (A); E6.5/Midstreak (MS) (B, F-G); E7.5/Early Bud (EB) (C, H); E7.5/Late Bud (LB) (D, I); and E7.5/Head Fold (HF) stages (E, J). (A-F) lateral views of whole mount RNA *in situ* hybridizations; (G-J) transverse sections at the levels indicated in (B-E); anterior is to the left. (E) Inset shows frontal view of *Bmp2* expression in anterior endoderm. (F) Two color *in situ* hybridizations to *Bmp2* (light blue) and *Cer1* or *brachyury* (purple). Size bars in A-E represent 50 microns. All, allantois; ant midl, anterior midline; em, embryonic; em mes, embryonic mesoderm; exem, extraembryonic; exem mes, extraembryonic mesoderm; OPC, open proamniotic canal; PS, primitive streak. See also Figures S1a and S1b.

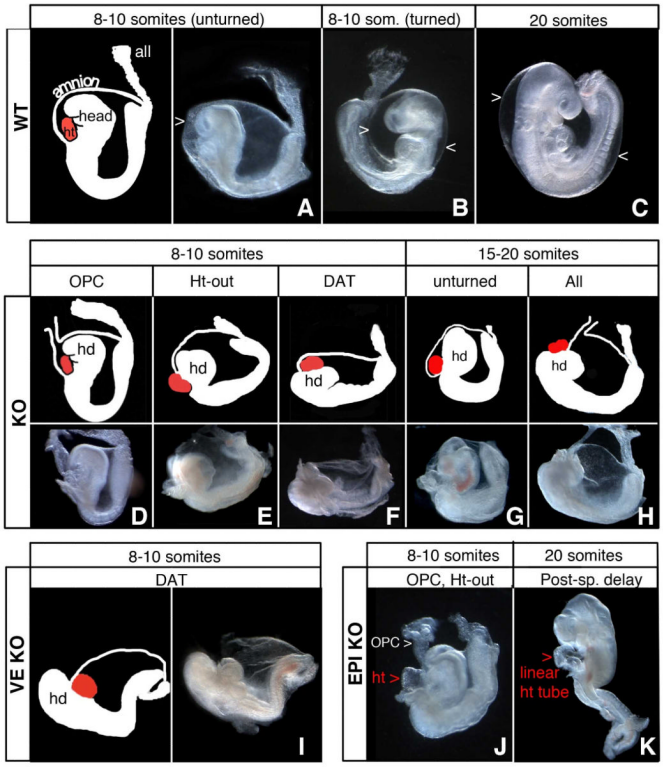

Figure 2. Lineage Specific Mutants Show Distinct and Complementary Functions for BMP2 expression in VE versus Epiblast-derivatives

(A-C) WT embryos show proper arrangement of head, heart, amnion and allantois before (A-B) and after (C) turning. In WT the heart resides ventral to the head and is looped; both the head and heart sit inside the amnion. (A-B) E8.5, 8-10 somite stage; (C) E9.5, 20 somite stage. >, amnion.

(D-H) KO embryos show a range of phenotypes including: (D) Open Proamniotic Canal (OPC); (E) Heart-outside the amnion (Ht-out); (F) Disorganized Anterior (DAT); (G) unturned; and (H) all four defects: OPC + Ht-out + DAT + unturned.

(I) VE-KO embryos display the DAT phenotype but not Ht-out or OPC.

(J-K) EPI-KO embryos display OPC and Ht-out but not DAT (J); 20+ somite stage EPI-KO embryos (K) develop somites, a closed neural tube, and eye and ear primordia, but contain an unlooped heart and remain unturned. all, allantois; hd, head; ht, heart;. See also Tables S2a and S2b.

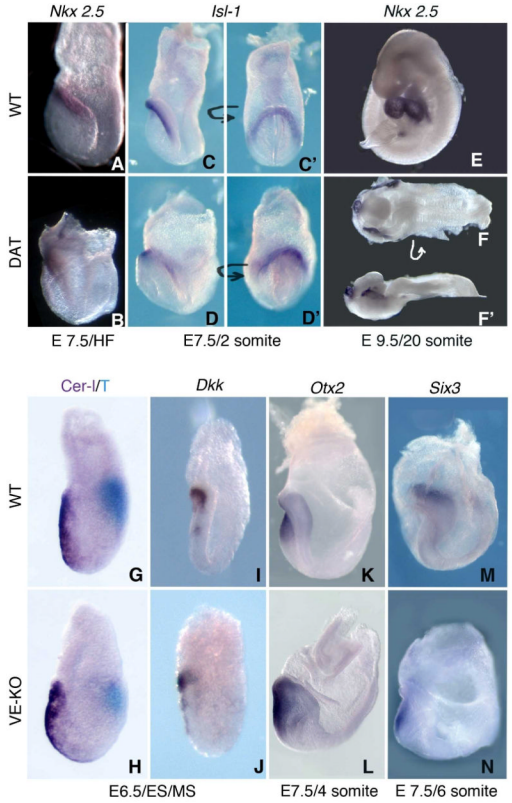

Figure 3. Head and Heart are specified in *Bmp2* Mutants

(A-F) WISH to markers for specification of cardiac mesoderm in WT and KO embryos. Lateral views of *Nkx2.5* stained HF stage (A-B) and 20 somite stage (E-F') WT (A, E) and KO embryos (B, F-F'). Dorsal view (F) and lateral view (F') of a disorganized anterior KO embryo showing partial cardia bifida. *Islet-1* (*Isl-1*) in 2 somite stage WT (C-C') and VE-KO (D-D') embryos; lateral views with anterior to the left (C-D); frontal/anterior views of the cardiac crescent (C'-D').

(G-N) WISH to markers for head specification in WT and VE-KO embryos. Lateral views of WT (G, I, K, M) and VE-KO (H, J, L, N) embryos stained for *Cer1* (purple) and *brachyury* (*T*, light blue) mRNA (G, H) and for *Dkk1* mRNA (I-J) at the ES/MS stage; stained for *Otx2* (K-L) at the 4 somite stage; and stained for *Six3* (M-N) at the 6 somite stage. See also Figure S3.

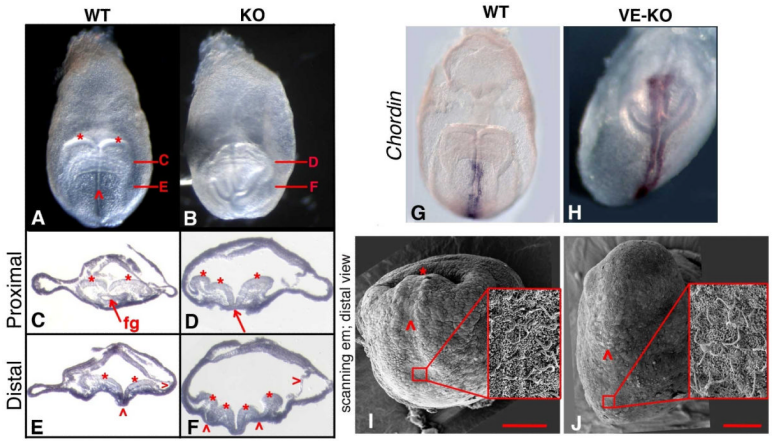

Figure 4. Disorganized Anterior KO Mutants Display Ectopic Neural Folds and Absence of the Anterior Intestinal Portal

(A-B) Frontal/anterior views of WT and KO 4 somite stage embryos. Two head folds (*) and a single neural groove (^) are evident in WT (A) but not in KO (B).

(C-F) Transverse sections at the regions indicated in A and B; anterior is downward. (C) Proximal WT section showing symmetrical head folds (*) and foregut (fg). (E) Distal WT section showing the two head folds (*), medial hinge point (^) and surface ectoderm (>). (D) Proximal KO section shows uneven head folds (*) and no gut tube (red arrow). (F) Distal KO section shows additional head folds (*), ectopic hinge points (^), surface ectoderm (>), and no gut tube.

(G-H) Frontal views of *Chordin* mRNA staining in early somite stage WT (G) and VE-KO (H) embryos.

(I-J) Scanning electron micrographs of distal views of WT (I) and VE-KO (J) early somite stage embryos: (I-J) node, red box and inset; midline (^); and anterior intestinal portal (*); 100 μm scale bar in red. See also Figure S4.

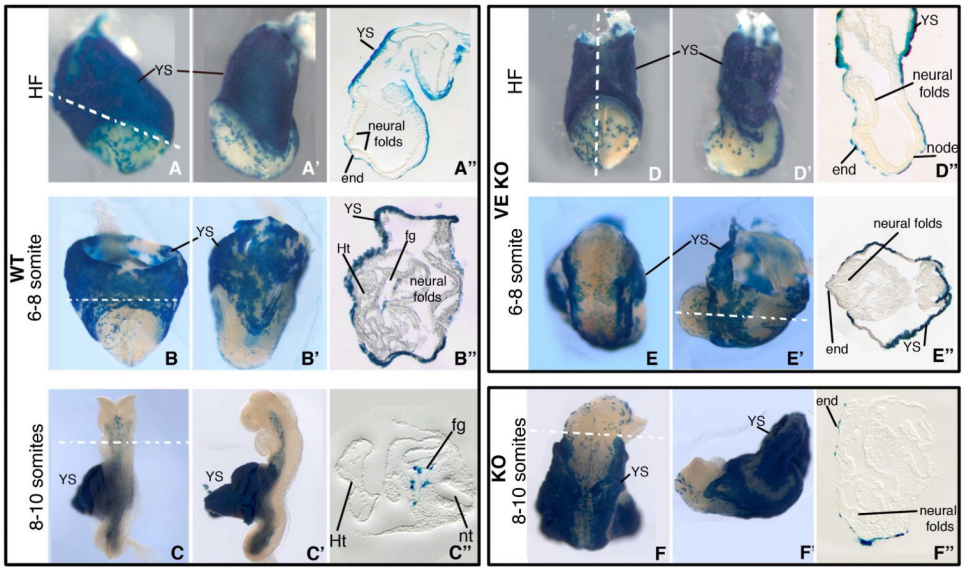

Figure 5. Visceral Endoderm Derivatives are integrated into the Primitive Gut of VE-KO and KO Embryos

(A-C, A'-C', A"-C") WT, (D-E, D'-E', D"-E") VE-KO, and (F, F', F") KO embryos carrying *Ttr::Cre* and *LacZR* transgenes show the position of VE derived cells (blue) in the yolk sac and developing gut tube. (A-C, D-F) Frontal view; (A'-C', D'-F') lateral view; (A"-C", D"-F") transverse sections of HF (A-A", D-D"), 6-8 somite (B-B", E-E") and 8-10 somite (C-C", F-F") stage embryos. end, endoderm; fg, foregut; Ht, heart; nt, neural tube; YS, yolk sac.

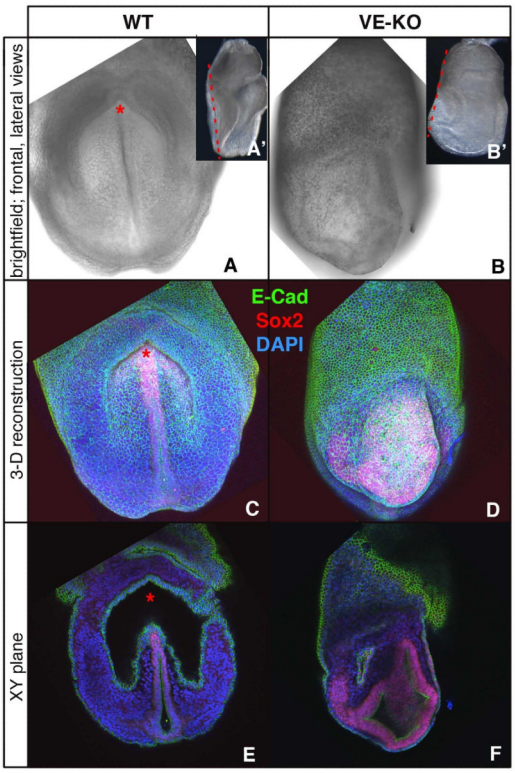

Figure 6. Ectopic Neural Folds at the Site of the Absent Foregut Invagination in Early-Somite Stage VE-KO Embryos

(A-B) Bright field views of WT (A, A') and VE-KO embryos (B, B'): frontal (A, B) lateral (A', B').

(C-D) 3-D reconstructed Z-Stacks of embryos in A and B stained with DAPI (blue) and with antibodies to E-Cad (green) and Sox2 (red).

(E-F) Frontal XY sections taken at the plane indicated by the red dashed lines in A' and B'.

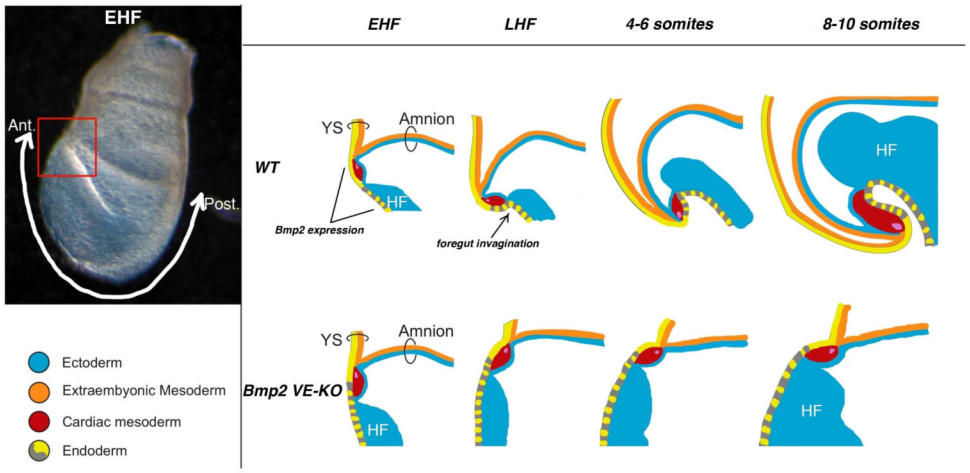

Figure 7. Foregut Invagination is Concurrent with Head/Heart Translocation

Left: Lateral view of an early head fold stage (EHF) mouse embryo highlighting anterior embryonic/extraembryonic junction (red box) and anterior-posterior axis (white arrow). Right: Schematic of anterior em/exem region through time in WT (top row) and *Bmp2* VE-KO mutant (bottom row) embryos. At EHF stages, in both WT and *Bmp2* mutant embryos, the junction of the yolk sac (YS), amnion, and heart lies anterior to the head folds (HF). By the 8-10 somite stage, WT head folds have translocated anterior to the YS/amnion/heart junction, but *Bmp2* mutant head folds remain posterior to the junction. In both WT and *Bmp2* VE-KO embryos, the yolk sac endoderm is comprised solely of visceral endoderm derivatives while the embryonic endoderm is comprised of derivatives from both visceral endoderm (yellow) and definitive endoderm (grey). BMP2 signals from the visceral endoderm are required for both foregut invagination and for translocation of head and heart. See also Video Abstract.